COMMUNICATION

ChemComm
www.rsc.org/chemcomm

Nanotectonic approach of the texturation of CeO_2 based nanomaterials†

Anne Bouchara,[a] Galo J. de A. A. Soler-Illia,[a] Jean-Yves Chane-Ching[b] and Clément Sanchez*[a]

[a] *Chimie de la Matière Condensée, UMR CNRS 7574, Université Pierre et Marie Curie 4, place Jussieu, 75252 Paris, France. E-mail: clems@ccr.jussieu.fr*

[b] *Rhodia Recherche, 52, rue de la Haie Coq, 93308 Aubervilliers, France*

Received (in Cambridge, UK) 5th March 2002, Accepted 19th April 2002
First published as an Advance Article on the web 7th May 2002

Original and homogeneous macrotextures shaped with coral-like, helical or macroporous sieves morphologies are obtained following a nanotectonic approach based on the template-directed assembly by poly-γ-benzyl-L-glutamate (PBLG) of organically functionalised CeO_2 crystalline nanoparticles.

Cerium oxide based catalysts are widely used as effective oxidation systems. These properties strongly depend on the nature of the metal centre and the crystallinity of the resulting oxide. Using crystalline nanoparticles (nano-building blocks = NBB) as the inorganic precursors allows retention of the electronic properties of CeO_2 for this type of application.[1] The NBB can be associated with different assembling strategies, thus allowing to build a great variety of architectures using organic–inorganic interfaces as templates.[2,3] The tuning of interactions between the surface of the NBB and the organic texturing agent are of paramount importance for the control of the texturation process.

In this work, we present the use of modified CeO_2 crystalline nanoparticles as NBB to obtain textured oxides[4,5] using a polypeptide (PBLG) as a template. PBLG is a polypeptide [Fig. 1(a)] that presents secondary protein-like structures such as α helix or β sheet-like in solvents as THF or DMF.[6,7]

The synthesis approach to integrate both components in a hybrid composite was based on tuning particle–template with template–template and particle–particle interactions (hydrophobic, hydrogen bonding or π–π[8] interactions) that can be adjusted by selective functionalisation of the nanoparticles. Hydrophobic interactions between nanoparticles and the phenyl groups of PBLG is attained by modifying the nanoparticle surface with alkyl groups. Phenyl functionalised nanoparticles favour π–π interactions with the phenyl group of the PBLG. Amine functionalised CeO_2 was also used to create hydrogen bonding with the ester group of the PBLG. Finally, a double functionalisation of the nanoparticles was achieved through the simultaneous surface capping by phenyl and amino groups.

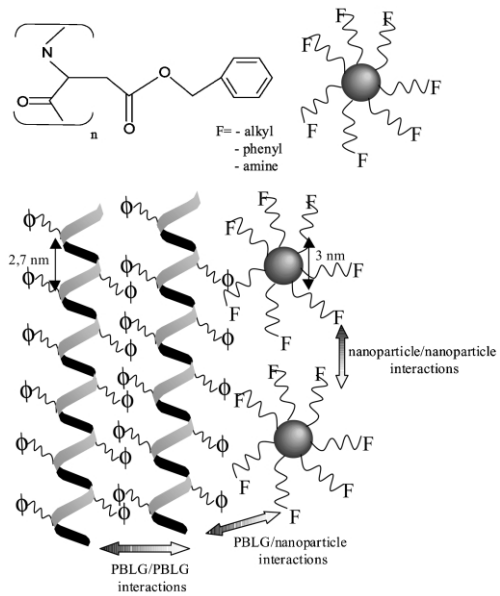

Fig. 1 a. PBLG formula and cartoon of functionalized nanoparticle **b**. Scheme of the possible interactions between the different building blocks (Φ = phenyl, F = any function alkyl, phenyl, amine).

† Electronic supplementary information (ESI) available: complete characterisation (FTIR, BET, EDS, TGA/DSC) available. See http://www.rsc.org/suppdata/cc/b2/b202316b/

A typical preparation of the powders can be described as follows: the CeO_2 hydrate‡ is dissolved in THF leading to a sol of monodisperse nanocrystalline particles, with size of about 3 nm as observed by TEM. This is in agreement with XRD information; dried sols exhibit broad patterns characteristic of crystalline CeO_2 particles, which size (calculated by Debye–Scherrer formula from the 111 peak) is 3 nm. Addition of a functionalised carboxylic acid (Table 1) leads to organic modification of the nanoceria surface. FTIR bands at 1302 and 1467 cm^{-1} (ESI)† correspond to antisymmetric and symmetric vibrations of the carboxylate groups. Their position and their splitting of 165 cm^{-1} are characteristic of bridging carboxylates. Caprylic acid, 5-phenylvaleric acid or 6-aminocaproic acid were used with ratios r = acid/CeO_2 ranging from 0.2 to 0.6. Thus, different functions can be imparted to the modified particles. PBLG was dissolved at 50 °C in THF with a total mass ratio ranging from 0.1 to 1%. The sol of organically modified CeO_2 nanoparticles was then slowly added to the PBLG solution under stirring. The molar ratio s = nanoparticles/PBLG was varied from 1 to 100. The obtained transparent solution was then placed in Petri dishes at ambient atmosphere for drying or was used to prepare thin films by dip-coating. After drying at room temperature, the morphology of the resulting xerogels was characterised by SEM and TEM.

Alkyl functionalised nanoparticles templated by PBLG lead to coral-like structures for s = 15 [Fig. 2(b)]. Similar morphologies were obtained by Caruso *et al.*[9] with amorphous TiO_2. In the present case the helical structure of PBLG is clearly altered. The helical morphology is however kept with doubly functionalised (amine and phenyl) particles in DMF for s = 15.

Phenyl functionalised nanoparticles lead to different morphologies depending on the ratio s. For $10 < s < 60$, helical morphology was obtained. By SEM, we detect helices of size 7 μm composed of smaller helices of size 1 μm [Fig. 2(c)]. The observation of these helices by TEM reveal a texture in the 6 nm size [Fig. 2(d)]. The π–π interactions between nanoparticles and PBLG seem to be effective and lead to an original morphology. Homogeneous morphologies are obtained for r = 0.2. Above s

Table 1 Morphologies associated to capping functions

Complexing group	Function	Morphology
COOH	C_7H_{14}	Coral-like
COOH	$Φ$-C_4H_8	Macroporous
COOH	$Φ$-C_4H_8	Helical
COOH	$Φ$-C_4H_8 + $H_2NC_5H_{10}$	Helical

DOI: 10.1039/b202316b

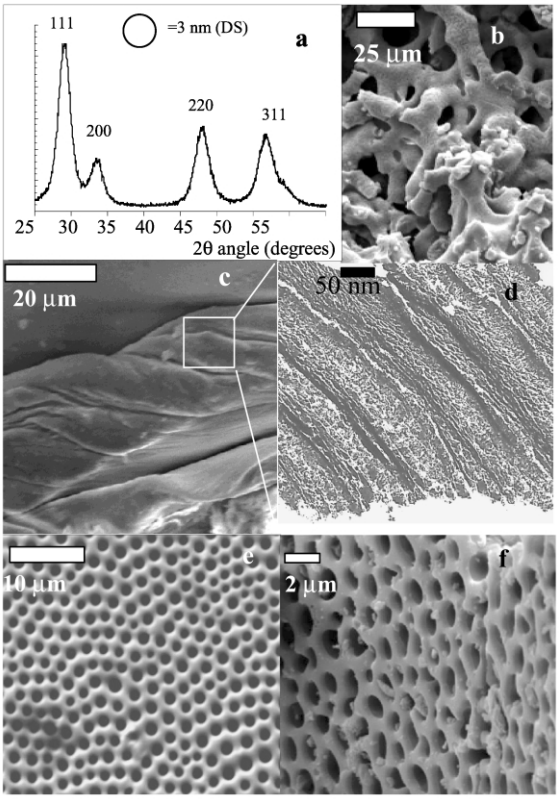

Fig. 2 (a) XRD pattern of 300 °C calcined CeO_2. (b) SEM image of the coral-like structure of a hybrid CeO_2/PBLG sample. (c) SEM and (d) TEM images of the helical structure of a calcined PBLG sample. (e) SEM image of a hybrid macroporous sample. (f) SEM image of a 500 °C calcined macroporous sample.

= 60, the solid exhibits macropores with diameters from 500 nm to 1 μm [Fig. 2(e) and (f)]. Such a regular morphology can be observed on very large domains of 500 μm and is reproducibly obtained. This morphology appears to be created at the surface of the bulk and seems to be associated with the solvent evaporation. Thin films prepared by dip-coating with these solutions also exhibit macropores. Varying the PBLG ratio allows control of the macropore size (ESI†). The variation of water/THF ratio allows either pores or microspheres to be obtained. The obtained morphologies are characteristic of phase separation by spinodal decomposition.[10,11]

PBLG can be removed by thermal treatment at rather low temperature with the aim of obtaining CeO_2 organic free materials. ATG measurements show a four step degradation of organic entities in the material (ESI†). The two first steps correspond to water and THF elimination, a third step at 200 °C is linked with the degradation of PBLG and the last step at 300 °C corresponds to the complete elimination of organics. The elimination of PBLG is followed by FTIR and confirmed by EDS (ESI†). Coral-like structures are retained after calcination at 300 °C. The macroporous samples are stable up to 500 °C as shown in Fig. 2(c). Helical structures remain after elimination of the PBLG at 300 °C as shown on SEM and TEM images in Fig. 2(c) and (d).

The specific areas (BET) for different calcination temperatures measured by N_2 adsorption at 77 K are reported in Table 2.

An optimum of specific surface area is reached at 300 °C, when the PBLG is eliminated. At 300 °C, the calcined samples exhibit a type I isotherm, which is characteristic of microporous materials (ESI†). The measured microporosity is due to the voids created upon aggregation of the nanoparticles. This process yields hierarchical porous materials presenting both micro and macro porosity with inorganic walls constituted of nano-crystalline cerium oxide particles as demonstrated by

Table 2 Crystallite sizes (Debye–Scherrer) and surface areas (BET)

Temperature/°C	Crystallite size/nm	Specific surface area/$m^2\ g^{-1}$
200	3	91
300	4	152
400	7	73
500	16	23
600	18	27

XRD [Fig. 2(a)]. For higher temperatures, the samples exhibit type III isotherms which are characteristic of macroporous materials (ESI†). The loss of microporosity is due to the sintering of the ceria nanoparticles, as shown in Table 2.

This original study demonstrates that a single parameter as *s* ratio allows a versatile tuning between a templating effect and phase separation. The control of the balance between these two processes allows to tailor diverse morphologies and textures.

The different morphologies obtained are likely related to the different interactions balance of components present in the system (polymer–polymer; polymer–surface capping agent, solvent–polymer, solvent–nanoparticles).

For $s > 60$, high water quantities are added. In this region, the phase segregation of submicrometer water droplets is the dominant texturing process. Phenyl capped NBB ceria dissolve in the polymer, and the resulting obtained material exhibits an ordered array of macropores. For lower *s* values, PBLG/PBLG interactions take over, leading to fiber-like materials. It is known that side-by-side association of PBLG molecules is favoured at long range by dipole–dipole interactions and at short range by side group interactions.[12] The helical structure is maintained in the appropriate solvent. Functionalised particles can dissolve between polymer threads leading to helical textured CeO_2 nanoparticles.

Nanotectonic approaches appear to be a biomimetic way to create new materials that keep the properties linked with the crystallinity of the particles. The synthesis method allows for the production of both gels and thin films with pores aligned perpendicularly to the surface. This versatile approach can be extended to other capping groups (functions such as thiol or aldehyde, morphology directors such as block copolymers, dendrimers) and to a great variety of controlled nanoparticle-based systems (TiO_2, ZrO_2, Al_2O_3,…).

Rhodia, CONICET and Fundación Antorchas are gratefully acknowledged for financial support.

Notes and references

‡ CeO_2 nanoparticles are obtained from the hydrate $CeO_2(HNO_3)_{0,5}(H_2O)_4$ delivered by Rhodia .

1 M. Fluytzani-Stephanopoulos, *MRS Bull.*, November 2001, 885.
2 C. Sanchez, G. J. de A. A. Soler-Illia, F. Ribot, T. Lalot, C. R. Mayer and V. Cabuil, *Chem. Mater.*, 2001, **13**, 3061.
3 (*a*) S. Mann, W. Shenton, M. Li, S. Connolly and D. Fitzmaurice, *Adv. Mater.*, 2000, **12**, 147; (*b*) F. A. Caruso, *Adv. Mater.*, 2001, **13**, 11; (*c*) J. H. Fendler, *Chem. Mater.*, 1996, **8**, 1616.
4 T. H. Galow, A. K. Boal and V. M. Rotello, *Adv. Mater.*, 2000, **12**, 576.
5 S. A. Davis, M. Beulmann, K. H. Rhodes, B. Zhang and S. Mann, *Chem. Mater.*, 2001, **13**, 3218.
6 P. Doty, J. H. Bradbury and A. M. Holtzer, *J. Am. Chem. Soc.*, 1956, **78**, 947.
7 T. Yang and P. Doty, *J. Am. Chem. Soc.*, 1957, **79**, 761.
8 R. Tamaki, K. Samura and Y. Chujo, *Chem. Commun.*, 1998, 1131.
9 R. Caruso, M. Antonietti, M. Giersig, H.-P. Hentze and J. Jia, *Chem. Mater.*, 2001, **13**, 1114.
10 K. Nakanishi, *J. Porous Mater.*, 1997, **4**, 67.
11 S. Kumon, K. Nakanishi and K. Hirao, *J. Sol–Gel Sci. Technol.*, 2000, **19**, 553.
12 A. Wada, *J. Polym. Sci.*, 1960, **45**, 145.